



## STRUCTURAL AND MICROSTRUCTURAL CHARACTERIZATION OF $\text{CuMo}_{(1-x)}\text{W}_x\text{O}_4$ ( $x \leq 0.12$ ) CERAMICS SINTERED BY SPARK PLASMA SINTERING

M. Benchikhil<sup>1, 2</sup>, R. El Ouatif<sup>1\*</sup>, S. Guillemet-Fritsch<sup>2</sup>, L. Er-Rakho<sup>1</sup>, B. Durand<sup>2</sup>

<sup>1</sup>Laboratoire de Physico-Chimie des Matériaux Inorganiques, Faculté des sciences Ain Chock, Hassan II University of Casablanca, B.P 5366 Maarif, Maroc.

<sup>2</sup>Institut Carnot CIRIMAT, CNRS Université de Toulouse, 118 route de Narbonne, 31062 Toulouse Cedex 9, France.

**KEYWORDS:** Spark plasma sintering (SPS), Chemical preparation, Structural phase transition, Molybdate, Tungsten.

### ABSTRACT

Cupric molybdate  $\text{CuMoO}_4$  is an interesting material due to their rich electrical, optical and magnetic properties. In this work, Solid solutions  $\text{CuMo}_{(1-x)}\text{W}_x\text{O}_4$  ( $x \leq 0.12$ ) were obtained by pyrolysis at 400 -700°C for 2 hours of a polymeric precursors elaborated by polymerizable complex method. For  $x \leq 0.075$ , they were isostructural with  $\alpha\text{-CuMoO}_4$  and for  $0.075 < x \leq 0.12$ , they were isostructural with  $\gamma\text{-CuMoO}_4$ . Spark Plasma Sintering (SPS) at 300°C for 5 min under an applied pressure of 200 MPa led to variety  $\text{CuMoO}_4\text{-III}$  for tungsten contents in the range 0.075-0.12.

### INTRODUCTION

In recent years, transition metal molybdates  $\text{AMoO}_4$  (with  $A = \text{Cu}^{2+}, \text{Ni}^{2+}, \text{Co}^{2+}, \text{Fe}^{2+}$ ) have been largely studied owing to their theoretical and practical interests. Especially, copper molybdate  $\text{CuMoO}_4$  has been studied extensively due to their excellent piezochromic, thermochromic and magnetic properties and their potential applications as oxidation catalysts in chemical and petrochemical processes [1-7]. Numerous authors have studied the temperature and pressure dependences of the optical, electrical and magnetic properties of  $\text{CuMoO}_4$  [7-11].

Several polymorphs of  $\text{CuMoO}_4$  have been reported in the literature [7,12], this depends on temperature and pressure as well as the synthesis conditions. The stable polymorph under standard conditions of temperature and pressure is triclinic  $\alpha\text{-CuMoO}_4$  (P1 space group) [7]. The  $\gamma\text{-CuMoO}_4$  phase (also  $P\bar{7}$ ) is stable below 200 K [7]. For temperatures above 840 K a polymorph of hexagonal symmetry,  $\beta\text{-CuMoO}_4$ , has been reported [13]. Both polymorphs  $\text{CuMoO}_4\text{-II}$  and  $\text{CuMoO}_4\text{-III}$  are high-pressure modifications with wolframite type structure, but remain stable at ambient conditions. They are isostructural to  $\text{CuWO}_4$  [14,15]. Furthermore the polymorph  $\varepsilon\text{-CuMoO}_4$  has recently been reported [12]. Moreover, the temperatures/pressures of transition are adjustable by chemical doping [4,7].  $\text{CuMoO}_4\text{-III}$ ,  $\text{CuMoO}_4\text{-II}$  and  $\varepsilon\text{-CuMoO}_4$  are antiferromagnetic at low temperatures whereas  $\alpha\text{-CuMoO}_4$  and  $\gamma\text{-CuMoO}_4$  do not show any magnetic ordering until 2K [5,12,13,15].

Numerous synthesis procedures of the molybdate  $\text{CuMoO}_4$  have been investigated: solid state reaction [13], mechano-synthesis [16], co-precipitation [17], pyrolysis [18], polyol method [19] and recently the polymerizable complex method [20,21]. This latter, allowing the control of the particles size, the composition and the homogeneity of powders [20-23], was chosen for the preparation of the solid solutions  $\text{CuMo}_{(1-x)}\text{W}_x\text{O}_4$  ( $x \leq 0.12$ ). Solid solutions  $\text{CuMo}_{(1-x)}\text{W}_x\text{O}_4$  were synthesized within the domain of solubility of tungsten in  $\text{CuMoO}_4$  ( $0 \leq x \leq 0.12$ ) and the corresponding dense ceramics were obtained by spark plasma sintering.

### EXPERIMENTAL PROCEDURES

The precursors were synthesized by the polymerizable complex method using the appropriate amounts of copper nitrate  $\text{Cu}(\text{NO}_3)_2 \cdot 3\text{H}_2\text{O}$  (Acros organics, 99.9%), ammonium molybdate  $(\text{NH}_4)_6\text{Mo}_7\text{O}_{24} \cdot 4\text{H}_2\text{O}$  (Sigma Aldrich, 99.8%), ammonium tungstate  $(\text{NH}_4)_{10}\text{W}_{12}\text{O}_{41} \cdot 5\text{H}_2\text{O}$  (Acros organics, 99.0%) and citric acid (Acros organics, 99.9%). The synthesis procedure was similar to that used for the preparation of not doped  $\alpha\text{-CuMoO}_4$  [20]. The precursors obtained were calcined under air for 2 hours at 420 or 700°C depending on their tungsten content.

The ceramics were prepared using both conventional sintering in air performed in a muffle furnace and by spark plasma sintering (SPS). For conventional sintering, discs were formed by uniaxial pressing at 25 bars at room temperature in the presence of an organic binder (Rhodoviol) so as to avoid the phenomenon of rolling. The green density of the pellet is ~ 61% of theoretical density. Pellets were sintered at 520-700°C for 2 h in air with a heating rate of 2.5 °C/min. SPS was carried out using a Dr. Sinter 2080 device from Sumitomo Coal Mining (Fuji Electronic Industrial, Saitama, Japan). The same processing parameters were used for all the compositions. The



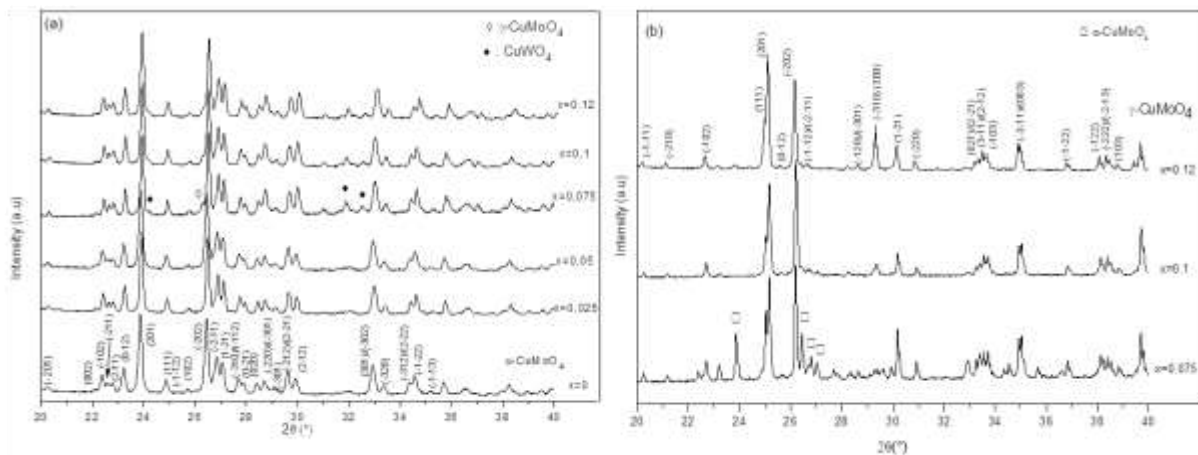
powder was placed in an 8 mm tungsten carbide die and then sintered at 300°C for 5 min under a pressure of 200MPa. The heating rate was set to 150°C/min.

The crystalline structure was investigated by X-ray diffraction analysis using a D4 Endeavor X-ray diffractometer ( $\text{CuK}\alpha = 0.154056 \text{ nm}$  and  $\text{CuK}\beta = 0.154044 \text{ nm}$ , operating voltage 40 kV and current 40 mA). The grain size and morphology of the powders and the microstructure of the sintered ceramics were observed with a scanning electron microscope (SEM, JEOL JSM 6400). The sintering behavior was studied by dilatometry (TMA Setsys 16/18) under air flow (heating rat =2.5 °C/min).

## RESULTS AND DISCUSSION

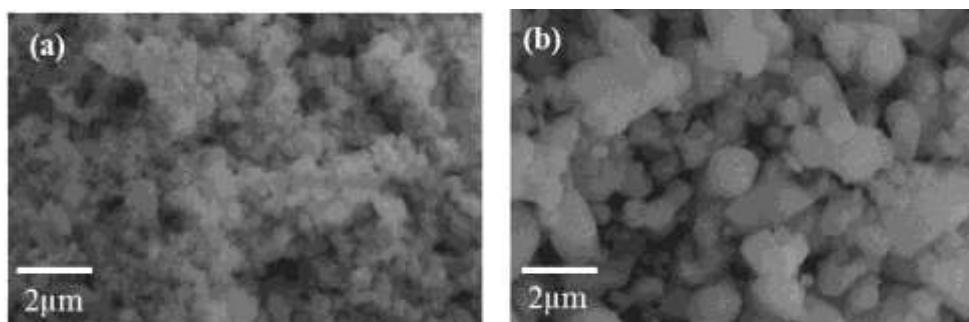
### Powders

Fig.1-a shows the measured XRD data for the samples calcined under air at 420 for 2 hours. For  $x \leq 0.075$ , all diffraction peaks are attributable to a phase triclinic isostructural with  $\alpha\text{-CuMoO}_4$  (JCPDS 073-0488). The XRD pattern shows no evidence of the presence of  $\gamma\text{-CuMoO}_4$ . For  $0.075 < x \leq 0.12$ , mixtures of three phases were identified:  $\alpha\text{-CuMoO}_4$ ,  $\gamma\text{-CuMoO}_4$  and  $\text{CuWO}_4$  (JCPDS 088-0269). The calcination temperature had to be raised up to 700 °C to obtain a pure solid solutions isostructural with  $\gamma\text{-CuMoO}_4$  (Fig.1-b).



**Fig.1. XRD patterns of  $\text{CuMo}_{(1-x)}\text{W}_x\text{O}_4$  oxides after calcination of xerogels at (a) 420 and (b) 700°C for 2h. Miller indices are indicated for  $\alpha\text{-CuMoO}_4$  (JCPDS 037-0488) and  $\gamma\text{-CuMoO}_4$  (JCPDS 088-0620) phases.**

The microstructures of solid solutions obtained by pyrolysis for 2h at 420 or 700°C were examined by scanning electron microscopy. The  $\alpha\text{-CuMo}_{0.95}\text{W}_{0.05}\text{O}_4$  solid solution was constituted of particles agglomerated with a poly-disperse size distribution (Fig. 2-a). These agglomerates are consisted in elongated or more or less spherical elementary grains with sizes in the range 0.1-0.2  $\mu\text{m}$  whereas the  $\gamma\text{-CuMo}_{0.88}\text{W}_{0.12}\text{O}_4$  solid solution was constituted of relatively spherical grains with sizes included in the range 0.5-2.0  $\mu\text{m}$  (Fig. 2-b).



**Fig.2. SEM micrographs of (a)  $\alpha\text{-CuMo}_{0.95}\text{W}_{0.05}\text{O}_4$  and (b)  $\alpha\text{-CuMo}_{0.88}\text{W}_{0.12}\text{O}_4$**

**Bulk ceramics**

3.2a for  $x \leq 0.05$

Fig. 3 shows the shrinking rates of the green compact  $\alpha\text{-CuMo}_{(1-x)}\text{W}_x\text{O}_4$  ( $x=0, 0.025$  and  $0.05$ ) powders via dilatometry under a constant heating rate of  $2.5^\circ\text{C}/\text{min}$ . As can be seen from Fig. 3, doping  $\text{CuMoO}_4$  powders with  $\text{W}^{6+}$  cations delays the densification at higher temperatures. Indeed, the densification starts at  $\sim 470$  and  $\sim 505^\circ\text{C}$  for  $x=0.025$  and  $x=0.05$  respectively, compared  $\sim 455^\circ\text{C}$  for pure  $\text{CuMoO}_4$ . The higher densification rates of pure  $\text{CuMoO}_4$  are obtained at  $525^\circ\text{C}$ , compared to  $560$  and  $600^\circ\text{C}$  for  $x=0.025$ , and  $x=0.05$  respectively. The density of  $\alpha\text{-CuMo}_{(1-x)}\text{W}_x\text{O}_4$  ( $x \leq 0.05$ ) ceramics is determined to be  $\sim 93\%$ .

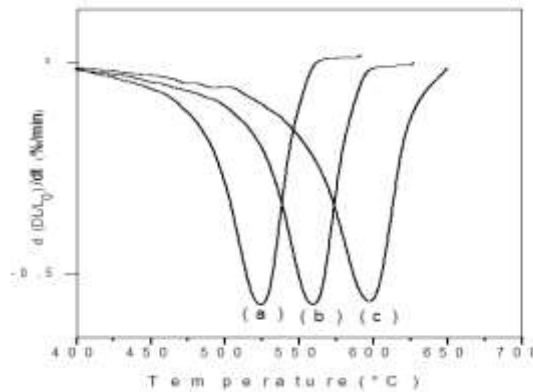


Fig.3. Shrinking rate versus temperature for  $\text{CuMo}_{(1-x)}\text{W}_x\text{O}_4$  ceramics, (a)  $x=0$ , (b)  $x=0.025$ , (c)  $x=0.050$

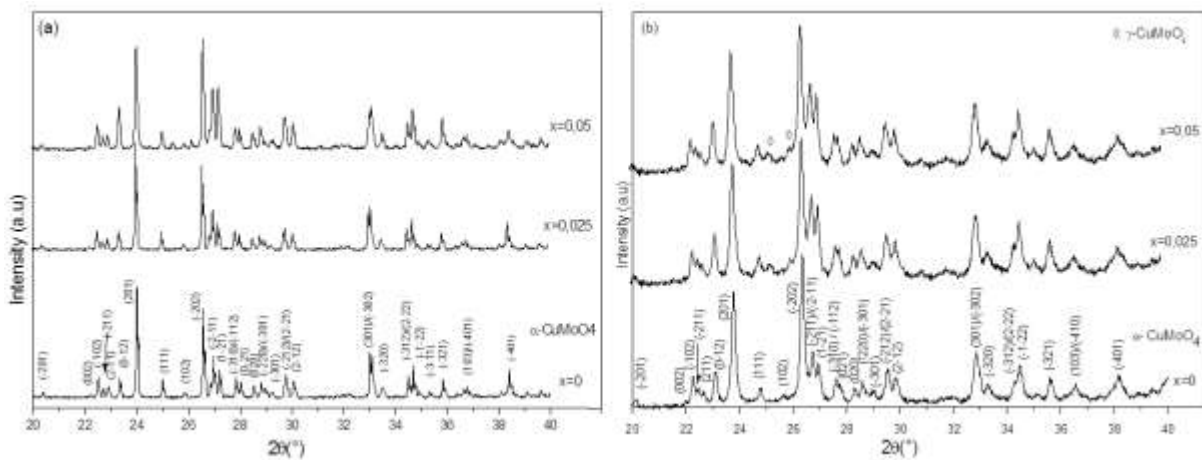


Fig.4. XRD patterns of  $\text{CuMo}_{(1-x)}\text{W}_x\text{O}_4$  ( $x=0, 0.025$  and  $0.05$ ): (a) conventionally sintered and (b) SPS sintered at  $300^\circ\text{C}$  for  $5$  min with an applied pressure of  $200$  MPa. Miller indices are indicated for a (JCPDS 037-0488) phase.

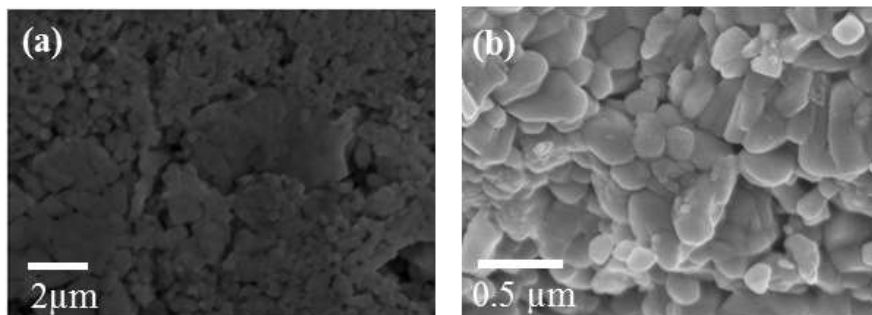


Fig.5. SEM micrographs of  $\text{CuMo}_{0.95}\text{W}_{0.05}\text{O}_4$ : (a) conventionally sintered at  $600^\circ\text{C}$  for  $2$  h, and (b) SPS sintered at  $300^\circ\text{C}$  for  $5$  min with an applied pressure of  $200$  MPa



The XRD patterns of the ceramics sintered by SPS at 300°C for 5 min under a pressure of 200 MPa showed, for  $x=0.025$  and  $x=0.05$ , that the molybdate  $\gamma$ -CuMoO<sub>4</sub> was formed beside  $\alpha$ -CuMoO<sub>4</sub> whereas those conventionally sintered are not modified by the thermal treatment (Fig.4).

The microstructures of the CuMo<sub>0.095</sub>W<sub>0.05</sub>O<sub>4</sub> ceramics prepared by the conventional sintering at 600°C for 2h and by spark plasma sintering (SPS) at 300°C for 5min with an applied pressure of 200MPa were examined by SEM. As shown in Fig. 5a, large pores were observed both at the grain boundaries and within the agglomerates in the conventionally sintered ceramics, indicating that the specimen was not really dense. For SPS samples (Fig. 5b), the grain sizes did not exceed 200 nm, with a relatively narrow granulometric distribution. Little residual porosity was observed. The broadness of the X-ray diffraction peaks of SPS sintered ceramic was comparable to that of the peaks of the non-sintered powder whereas the peaks of the conventionally sintered ceramic were significantly narrower (Fig.4). The SEM micrographs (Fig.5) are confirmed, i.e. on the contrary of conventional route, the SPS allows the limitation of the grain growth.

3.2b for  $0.075 < x \leq 0.12$

In order to better understand the sintering behavior of  $\gamma$ -CuMo<sub>(1-x)</sub>W<sub>x</sub>O<sub>4</sub> ( $0.075 < x \leq 0.12$ ) powders, dilatometry experiments was performed on the  $\gamma$ -CuMo<sub>0.88</sub>W<sub>0.12</sub>O<sub>4</sub> powder (Fig. 6). The dilatometric curve is characteristic of a sintering process in several stages. The shrinkage starts around 450 °C and ends after about two hour at 700 °C

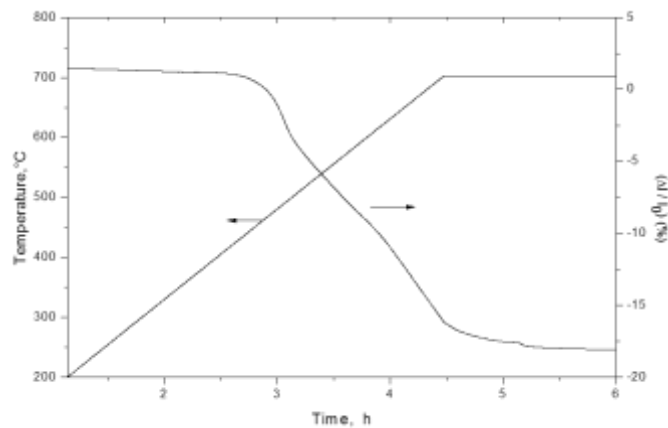


**Fig.6. Dilatometric behavior of CuMo<sub>0.88</sub>W<sub>0.12</sub>O<sub>4</sub>**

The ceramics obtained after sintering at 700°C for 2 hours and by SPS at 300° C for 5 min under a pressure of 200MPa were characterized by X-ray diffraction analysis (Fig.7) and by SEM (Fig. 8). All the peaks of X-ray diffraction patterns of CuMo<sub>(1-x)</sub>W<sub>x</sub>O<sub>4</sub> ( $0.075 < x \leq 0.12$ ) were indexed in a triclinic lattice with the space group P $\bar{1}$ , whatever the sintering procedure (Fig.7). The polymorphic form was dependent upon the sintering procedure. For conventional sintering, the solid solutions were isostructural with  $\alpha$ -CuMoO<sub>4</sub> whereas for SPS they were isostructural with CuMoO<sub>4</sub>-III (JCPDS 077-0699). In both cases,  $\gamma$ -CuMoO<sub>4</sub> appeared as minor structure.

The ceramics conventionally sintered at 700 °C for 2h were consisted of grains sized in the range 1-5 $\mu$ m and abnormal growth of some grains are observed (Fig. 8a). The sample sintered by SPS at 300°C for 5min presents much denser microstructure with largely grown platelets (Fig. 8b).



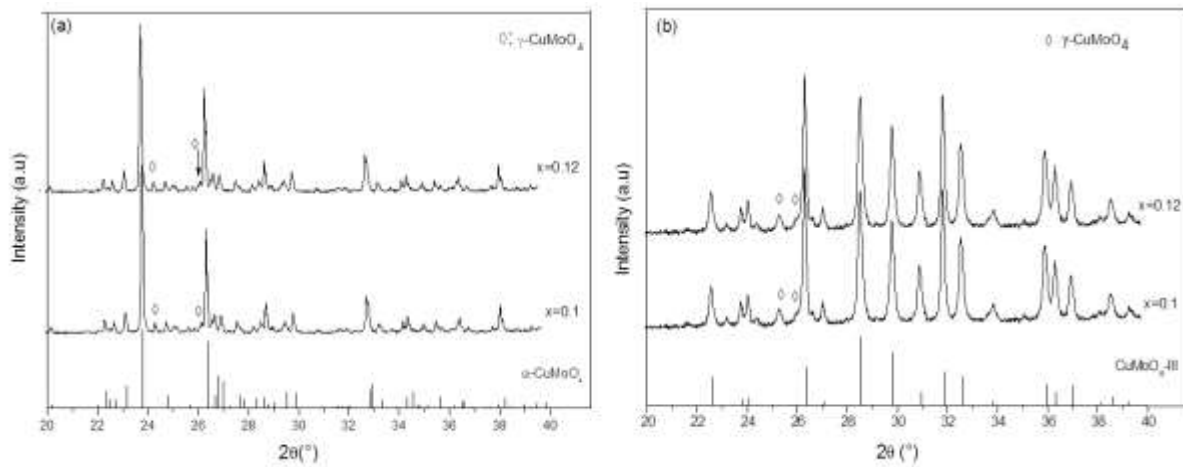


Fig.7. XRD patterns of  $\text{CuMo}_{(1-x)}\text{W}_x\text{O}_4$  (with  $x=0.1$  and  $0.12$ ): (a) conventionally sintered at  $700\text{ }^\circ\text{C}$  for 2 h, and (b) SPS sintered at  $300\text{ }^\circ\text{C}$  for 5 min with an applied pressure of 200 MPa.

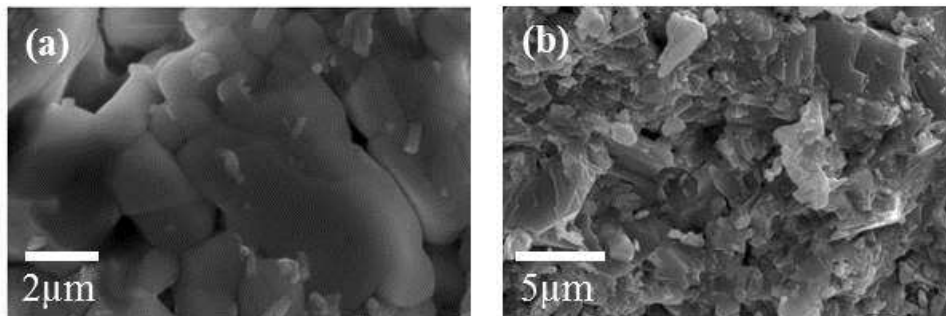


Fig.8. SEM micrographs of  $\text{CuMo}_{0.88}\text{W}_{0.12}\text{O}_4$ : (a) conventionally sintered at  $700\text{ }^\circ\text{C}$  for 2 h, and (b) SPS sintered at  $300\text{ }^\circ\text{C}$  for 5 min with an applied pressure of 200 MPa

## CONCLUSION

W-substituted  $\text{CuMoO}_4$  compounds,  $\text{CuMo}_{(1-x)}\text{W}_x\text{O}_4$  ( $0 \leq x \leq 0.12$ ), were obtained by pyrolysis at temperature in the range  $420\text{--}700\text{ }^\circ\text{C}$  for 2 hours of a gels prepared by the polymerizable complex method. For  $x \leq 0.075$ , they were isostructural to  $\alpha\text{-CuMoO}_4$  whereas, for  $0.075 < x \leq 0.12$ , they were isostructural to  $\gamma\text{-CuMoO}_4$ . Spark plasma sintering at  $300\text{ }^\circ\text{C}$  for 5 min under a pressure of 200 MPa led to variety  $\text{CuMoO}_4\text{-III}$  for tungsten contents in the range  $0.075\text{--}0.12$ .

## ACKNOWLEDGMENTS

This work was supported by two French-Moroccan projects: Volubilis Partenariat Hubert Curien (PHC no. MA 09 205) and Projet de Recherches Convention Internationale du CNRS (CNRS-CNRST no w22572).

## REFERENCES

1. L.A. Palacio, A.Echavari, L. Sierra and E. A. Lombardo, "Cu, Mn and Co molybdates derived from novel precursors catalyze the oxidative dehydrogenation of propane," in *catal. Today*, vol.107-108, pp.338-345, 2005.
2. N.V. Lebukhova, V.S. Rudnev, P.G. Chigrin, I.V. Lukiyanichuk, M.A. Pugachevsky, A.J. Ustinov, E.A. Kirichenko, and T.P. Yarovaya, "The nanostructural catalytic composition  $\text{CuMoO}_4/\text{TiO}_2+\text{SiO}_2/\text{Ti}$  for combustion of diesel soot," in *Surf. Coat.Tech.*, vol. 231, pp. 144-148,2013.
3. M.D. Ward, J.F. Brazdil, S.P. Mehandru and A.B. Anderson, "Methane photoactivation on copper molybdate: an experimental and theoretical study," in *J. Phys. Chem.*, vol.91, pp. 6515- 6521,1987.
4. I. Yanasen, T. Mizuno and H. Kobayashi, "Structural phase transition and thermochromics behavior of synthesized W substituted  $\text{CuMoO}_4$ ," in *Ceram. Int.*, vol.39, issue 2, pp. 2059-2064, 2013.



5. H. J. Koo and M.H. Whangbo, "Spin Dimer Analysis of the Anisotropic Spin Exchange Interactions in the Distorted Wolframite-Type Oxides  $\text{CuWO}_4$ ,  $\text{CuMoO}_4$ -III, and  $\text{Cu}(\text{Mo}_{0.25}\text{W}_{0.75})\text{O}_4$ ," in *Inorg. Chem.*, vol. 40, issue 9, pp. 2161-2169, 2001.
6. B.C. Schwarz, H. Ehrenberg, H. Weitzel and H. Fuess, "Investigation on the influence of particular structure parameters on the anisotropic spin-exchange interactions in the distorted Wolframite-type oxides  $\text{Cu}(\text{MoxW}_{1-x})\text{O}_4$ ," in *Inorg. Chem.*, vol. 46, pp. 378-380, 2007.
7. M. Wiesmann, H. Ehrenberg, G. Miehe, T. Peun, H. Weitzel and H. Fuess, "p-T Phase Diagram of  $\text{CuMoO}_4$ ," in *J. Solid State Chem.*, vol. 132, issue 1, pp. 88-97, 1997.
8. G. Mul, J.P.A. Neeft, F. Kapteijn, M. Makkee and J.A. Moulijn, "Soot oxidation catalyzed by a Cu/K/Mo/Cl catalyst: evaluation of the chemistry and performance of the catalyst," in *Appl. Catal. B*, vol. 6, issue 4, pp. 339-352, 1995.
9. J. Haber, T. Machej, L. Ungier and J. Ziolkowski, "ESCA studies of copper oxides and copper molybdates," in *J. Solid State Chem.*, vol. 25, pp. 207-218, 1978.
10. G. Steiner, R. Salzer and W. Reichelt, "Temperature dependence of the optical properties of  $\text{CuMoO}_4$ ," in *Fresenius J. Anal. Chem.*, vol. 370, pp. 731-734, 2001.
11. M. Benchikhi, R. El Ouatib, L. Er-Rakho, S. Guillemet Fritsch, B. Durand, F. Olivie and K. Kassmi, "Morphological and electric characterizations of a nanometric material  $\alpha$ - $\text{CuMoO}_4$  for photovoltaic application," in *J. Mater. Environ. Sci.*, vol. 4, issue 2, pp. 504-509, 2013.
12. J. Baek, A.S. Sefat, D. Mandrus and P. Shiv Halasyamani, "A New Magnetically Ordered Polymorph of  $\text{CuMoO}_4$ : Synthesis and Characterization of  $\epsilon$ - $\text{CuMoO}_4$ ," in *Chem. Mater.*, vol. 20, issue 12, pp. 3785-3787, 2008.
13. H. Ehrenberg, H. Weitzel, H. Paulus, M. Wiesmann, G. Wltschek, M. Geselle and H. Fuess H., "crystal structure and magnetic properties of  $\text{CuMoO}_4$  at low temperature ( $\gamma$ -phase)," in *J. Phys. Chem.*, vol. 58, issue 1, pp. 153-160, 1997.
14. A. W. Sleight, "High pressure  $\text{CuMoO}_4$ ," in *Mater. Res. Bull.*, vol. 8, pp. 863-866, 1973.
15. H. Ehrenberg, M. Wiesmann, J. Garcia-Jaca, H. Weitzel and H. Fuess, "Magnetic structures of the high-pressure modifications of  $\text{CoMoO}_4$  and  $\text{CuMoO}_4$ ," in *J. Magn. Magn. Mater.*, vol. 182, pp. 292-303, 1998.
16. D. Klissurski, R. Iordanova, M. Milanova, D. Radev and S. Vassilev, "Mechanochemically Assisted Synthesis of Cu (II) Molybdate," in *CR Acad. Bulgare Sci.*, vol. 56, pp. 39-42, 2003.
17. S. Mitchell, A. Gomez Aviles, C. Gardner and W. Jones, "Comparative study of the synthesis of layered transition metal molybdates," in *J. Solid State Chem.*, vol. 183, pp. 198-207, 2010.
18. K.S. Makarevich, N.V. Lebukhova, P.G. Chigrin and N.F. Karpovich, "Catalytic Properties of  $\text{CuMoO}_4$  Doped with Co, Ni, and Ag," in *Inorg. Mater.*, vol. 46, issue 12, pp. 1494-1499, 2010.
19. P. Schmitt, N. Brem, S. Schunk and C. Feldmann, "Polyol-Mediated Synthesis and Properties of Nanoscale Molybdates/Tungstates: Color, Luminescence, Catalysis," in *Adv. Funct. Mater.*, vol. 21, issue 16, pp. 3037-3046, 2011.
20. M. Benchikhi, R. El Ouatib, S. Guillemet Fritsch, J.Y. Chane Ching, L. Er-rakho and B. Durand, "Sol-gel synthesis and sintering of submicronic copper molybdate ( $\alpha$ - $\text{CuMoO}_4$ ) powders," in *Ceram. Int.*, vol. 40, issue 4, pp. 5371-5377, 2014.
21. M. Benchikhi, R. El Ouatib, L. Er-Rakho, S. Guillemet Fritsch, B. Durand and K. Kassmi, "Influence of chelating agent on the morphological properties of  $\alpha$ - $\text{CuMoO}_4$  powder synthesized by sol-gel method," in *J. Mater. Environ. Sci.*, vol. 6, issue 12, pp. 3470-3475, 2015.
22. S.M. Montemayor, L.A. García Cerda and J.R. Torres-Lubián, "Preparation and characterization of cobalt ferrite by the polymerized complex method," in *Mater. Lett.*, vol. 59, issues 8-9, pp. 1056-1060, 2005.
23. H. Lakhlifi, M. Benchikhi, R. El Ouatib, L. Er-Rakho, S. Guillemet Fritsch and B. Durand, "Synthesis and physicochemical characterization of pigments based on molybdenum «  $\text{ZnO-MoO}_3: \text{Co}^{2+}$  », " in *J. Mater. Environ. Sci.*, vol. 6, issue 12, pp. 3465-3469, 2015.